Dalton Transactions

Cite this: *Dalton Trans.*, 2012, **41**, 1889

www.rsc.org/dalton

PAPER

Coordination induced fluorescence enhancement and construction of a Zn_3 constellation through hydrolysis of ligand imine arms†

Avijit Sarkar,[a] Aloke Kumar Ghosh,[a] Valerio Bertolasi[b] and Debashis Ray*[a]

Received 22nd July 2011, Accepted 27th October 2011
DOI: 10.1039/c1dt11390a

The phenoxido and alkoxido bridged neutral Zn_3 complex $[Zn_3(\mu\text{-}H_2bemp)_2(\mu_3\text{-}emp)_2]$ (**1**), with an angular $Zn_3(\mu\text{-}OPh)_2(\mu\text{-}OEt)_2$ core and capping nitrogen donors, was synthesized *via* simultaneous chelation-*cum*-bridging of the parent and hydrolysed ligands. Zinc(II) coordination triggered the solution phase imine (C═N) bond hydrolysis of H_3bemp (2,6-bis-[(2-hydroxyethylimino)methyl]-4-methylphenol) and yielded the unexpected angular trinuclear Zn(II) complex **1**, having structural similarity with the Zn_3 active site of P1 nuclease. H_3bemp also displays a zinc(II) selective chelation-enhanced fluorescence response from strong metal ion coordination. Complexation of zinc(II) with H_3bpmp (2,6-bis-[(3-hydroxypropylimino)methyl]-4-methylphenol), a close analogue of H_3bemp, instead provides only mononuclear $[Zn(H_2bpmpH^N)_2](ClO_4)_2\cdot 2H_2O$ (**2**·$2H_2O$) (H^N is the proton attached to an imine nitrogen atom) of two zwitterionic ligands, generated through a kind of coordination driven *acid–base* reaction, without showing any aggregation reaction. As the sole metal–organic precursor, both the complexes under pyrolytic conditions give ZnO nano structures of two morphologies.

Introduction

This study combines the areas of zinc ion based fluorescence sensors and hydrolase activity of coordinated zinc ions for multimetallic constellation formation. Zinc is an essential element for humans and plays several important roles in a variety of biological processes. Coordinating ligand and small bridging group dependent self-assembly and control of the nuclearity of metal complexes have received intense interest in recent years. Phenolate group based binucleating compartmental ligands are known to provide dinuclear and tetranuclear complexes depending upon the versatility of the central and terminal bridging groups.[1] The formation of trinuclear complexes is mostly dominated by the involvement of nucleating oxo/hydroxo groups and terminal oximate type ligand bridges.[2] The synthesis and characterization of trinuclear complexes have attracted considerable interest following the identification of the Zn_3 motif in P1 nuclease[3] and phospholipase C,[4] and the Zn_2Mg core in alkaline phosphatase[5] (Scheme 1). The search for ligand systems responsible for the constellation of zinc(II) ions has been an active area of research, particularly due to the involvement of zinc(II) in neurobiology.[6] An acyclic tricompartmental tris-phenolate macrocyclic ligand was seen to generate a trinuclear complex.[7] The reactions of ligands bearing hydrolysable imine groups with zinc salts are of interest because the zinc ion is known to play an important role in several hydrolytic reactions due to its Lewis acidity, flexible coordination geometry, intermediate hard-soft behavior and rapid ligand exchange.[8] Multidentate phenoxide centered binucleating ligands[9] having flexible side-arms are known to provide bimetallic and tetrametallic structures.[10] In a specific reaction conditions and in the presence of other ancillary bridging ligands such a binucleating ligand can lead to the formation of transition metal ion aggregates from the involvement of truncated ligand systems and ligand hydrolysis assisted assemblage reaction.[11] The formation of an angular Zn_3 constellation from

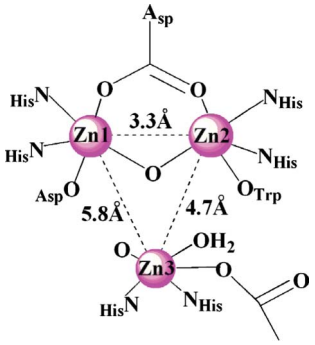

Scheme 1 An illustration of the trinuclear zinc active site of P1 nuclease.

[a]*Department of Chemistry, Indian Institute of Technology, Kharagpur 721 302, India. E-mail: dray@chem.iitkgp.ernet.in; Fax: 91-3222-82252; Tel: 03222-283324*
[b]*Dipartimento di Chimica e Centro di Strutturistica Diffrattometica, Università di Ferrara, via Borsari 46, 44100 Ferrara, Italy*

† Electronic supplementary information (ESI) available: Crystallographic data in CIF, Scheme S1 and Fig. S1–S22. CCDC reference numbers for complexes **1** and **2**·$2H_2O$ are 795505 and 795506, respectively. For ESI and crystallographic data in CIF or other electronic format see DOI: 10.1039/c1dt11390a

the coordination and partial hydrolysis of the Schiff base ligand 2,6-bis-[(2-hydroxyethylimino)-methyl]-4-methylphenol (H_3bemp; Scheme 2) is achieved from the incorporation of both five and six-coordinated metal ion centers. The zinc center is known to show extraordinary flexibility in the coordination geometry and can adopt distorted geometries.[12] Another important aspect of the zinc(II) coordination chemistry of Schiff base ligands is coordination induced hydrolysis of imine groups,[13] similar to the behaviour of zinc(II) bearing metallo-β-lactamases.[14] This is the first report of any Zn_3 complex bearing a central hexacoordinated zinc(II) center flanked by two pentacoordinated zinc(II) ions in an angular arrangement. Zwitterionic ligands having negatively charged donor atoms and positively charged remote centers are capable of binding both a metal ion and its accompanying anions leading to the selective anion binding property.[15]

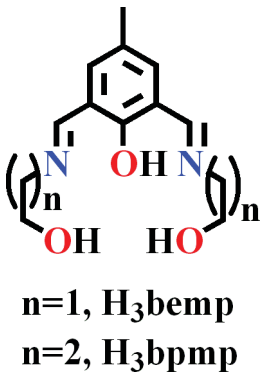

Scheme 2 Ligands H_3bemp and H_3bpmp.

We have focused our attention to explore the reactions of H_3bemp and H_3bpmp with $Zn(ClO_4)_2{\cdot}6H_2O$ for coordination assisted ligand hydrolysis and zwitterionic complex formation. The chelating arm dependent aggregation ability of H_3bemp has been exploited here in $[Zn_3(H_2bemp)_2(emp)_2]$ (**1**) and the mononuclear complex $[Zn(H_2bpmpH^N)_2](ClO_4)_2{\cdot}2H_2O$ (**2**·$2H_2O$). Most probably the zwitterionic form of H_3bemp with dangling ligand arms is prone to hydrolysis in the presence of Zn^{2+} (Scheme 3).

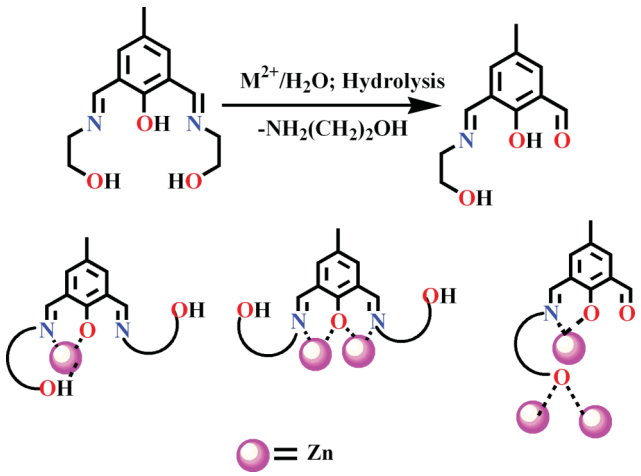

Scheme 3 Zn(II) coordination triggered partial hydrolysis of H_3bemp (above) and three different types of binding behaviors of H_3bemp and H_3bpmp (below).

The study presented in this paper provides new examples of ligands for the exclusive formation of mono or trinuclear complexes of zinc(II) depending on the size of the ligand side arms. Studies on the fluorescent properties of these two ligands show that the emission intensity increases significantly upon addition of various concentrations of Zn^{2+}, while the introduction of other transition metal ions and biologically significant metal ions causes the intensity to be either unchanged or weakened.

Experimental

Materials and physical methods

The chemicals used were obtained from the following sources: zinc carbonate from Universal Laboratory (India), ethanolamine (2-amino ethanol) from S.D. Fine Chem (India), 3-amino-1-propanol from Aldrich Chemical Co. Inc. 2,6-Diformyl-4-methylphenol (2-hydroxy-5-methyl-benzene-1,3-dicarbaldehyde) was prepared following a literature procedure.[16] All other chemicals and solvents were reagent grade materials and were used as received without further purification. The elemental analyses (C, H, N) were performed with a Perkin-Elmer model 240 C elemental analyzer. Fourier transform infrared (FT-IR) spectra were recorded on a Perkin-Elmer RX1 spectrometer. Solution electrical conductivity measurements and electronic spectra were carried out using a Unitech type U131C digital conductivity meter with a solute concentration of about 10^{-3} M and a Shimadzu 1601 UV-vis-NIR spectrophotometer using 1 cm quartz cell pairs. The fluorescence spectra were measured using a Hitachi F-7000 spectrofluorimeter.

Synthesis

2,6-Bis-[(2-hydroxy-ethylimino)-methyl]-4-methyl-phenol (H_3bemp). The Schiff base was prepared from the single step condensation reaction of 2,6-diformyl-4-methylphenol (1.0 g, 6.1 mmol) and 2-aminoethanol (0.74 g, 12.2 mmol) in MeOH (40 mL) under reflux for 1 h, as reported previously.[17]

2,6-Bis-[(3-hydroxy-propylimino)-methyl]-4-methyl-phenol (H_3bpmp). To a MeOH solution (20 mL) of 2,6-diformyl-4-methylphenol (1.0 g, 6.1 mmol), 3-amino-1-propanol (0.91 g, 12.2 mmol) was added in air at room temperature (28 °C) and stirred for 2 h to give an orange colored gummy product after complete evaporation of solvent in air for 12 h. The gummy product thus obtained was next used for complexation reaction. Crude yield: 1.32 g (78%).

$[Zn_3(H_2bemp)_2(emp)_2]$ (1). To a MeOH solution (20 mL) of H_3bemp (0.335 g, 1.33 mmol), neat NEt_3 (0.278 mL, 0.202 g, 2.00 mmol) was added dropwise with magnetic stirring during 15 min. After 0.5 h, a MeOH solution (10 mL) of $Zn(ClO_4)_2{\cdot}6H_2O$ (0.372 g, 1 mmol) was slowly added to the previous solution during 10 min and the resulting yellow solution was stirred for 1 h. The light yellow solid was separated from the resulting yellow solution on solvent evaporation in air. Filtration of the reaction mixture gives a yellow solid, which is isolated, washed with cold MeOH, and dried under vacuum over P_4O_{10}. The yellow single crystals suitable for single-crystal X-ray analysis were obtained from a saturated MeOH solution after 6 d. Yield: 0.337 g, 61%. Anal. calcd for $Zn_3C_{48}H_{56}N_6O_{12}$ (1105.10 g mol^{-1}); C 52.11, H 5.10, N 7.60. Found: C 52.05, H 4.95, N 7.54. ^{1}H NMR

(400 MHz, DMSO-d^6): δ = 2.097 (t, 2H), 2.184 (s, 3H), 2.239 (s, 3H), 3.570 (t, 6H), 3.642 (m, 4H), 3.570 (t, 2H), 7.456 (m, 4H), 8.359 (s, 3H), 10.36 (s, 1H). Selected FT-IR bands: (KBr, cm^{-1}, br = broad, vs = very strong, s = strong, m = medium) 3421 (br), 1636 (vs), 1457 (vs), 1233 (s), 1087 (s), 974 (s), 842 (m), 765 (s), 740 (s), 699 (s) 530 (s). Molar conductance, Λ_M: (MeOH solution) 6 Ω^{-1} cm^2 mol^{-1}.

[Zn(H$_2$bpmpH^N)$_2$](ClO$_4$)$_2$·2H$_2$O (2·2H$_2$O). To the MeOH solution (20 mL) of H$_3$bpmp (0.278 g, 1.00 mmol) a MeOH solution (10 mL) of Zn(ClO4)2·6H$_2$O (0.186 g, 0.50 mmol) was added slowly followed by NEt$_3$ (278 mL, 0.202 g, 2.00 mmol) and stirred for 1 h at room temperature. The solvent was evaporated in air to give an orange solid, which was isolated, washed with cold methanol, and dried under vacuum over P$_4$O$_{10}$. The orange single crystals suitable for single-crystal X-ray analysis were obtained from MeOH solution after 8 d. Yield: 0.153 g, 36%. Anal. calcd for Zn$_1$C$_{30}$H$_{46}$N$_4$O$_{16}$ (855 g mol^{-1}): C 42.14, H 5.42, N 6.55. Found: C 42.10, H 5.36, N 6.46. ^{1}H NMR (400 MHz, DMSO-d^6): δ = 1.792 (m, 4H), 2.239 (s, 3H), 2.484 (t, 2H), 3.546 (t, 4H), 3.643 (m, 4H), 7.585 (t, 2H), 8.296 (s, 2H). Selected FTIR bands: (KBr, cm^{-1}, br = broad, vs = very strong, s = strong, m = medium) 3420 (br), 1653 (vs), 1540 (vs), 1540 (vs), 1193 (s), 1088 (s), 625 (m). Molar conductance, Λ_M: (MeOH solution) 192 Ω^{-1} cm^2 mol^{-1}.

Results and discussion

Synthesis and characterization

The Schiff base 2,6-bis-[(2-hydroxy-ethylimino)-methyl]-4-methylphenol (H$_3$bemp) and 2,6-bis-[(3-hydroxy-propylimino)-methyl]-4-methylphenol (H$_3$bpmp) were prepared (Scheme S1 in the ESI†) following a literature procedure,[17] and their reactions with zinc(II) salts have been investigated, as summarized in Scheme 4. When the reaction of Zn(ClO$_4$)$_2$·6H$_2$O was carried out with H$_3$bemp in CH$_3$OH in presence of NEt$_3$ as base, **1** was obtained. Several H$_3$bemp/Zn/NEt$_3$ ratios were explored, and we report here the optimized one that gave a clean and characterizable product in high yield. At room temperature, complex **1** is easily isolated by stirring a methanolic solution of

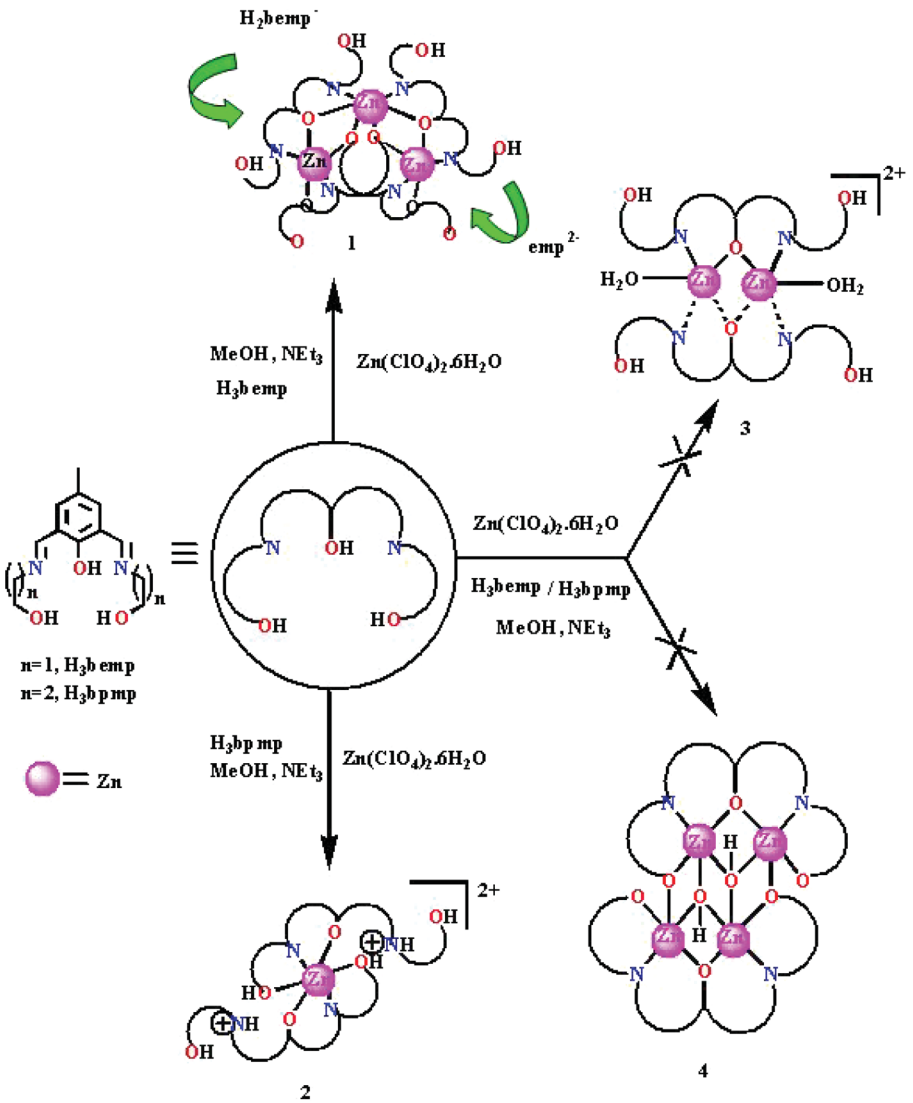

Scheme 4 Other possibilities for di and tetranuclear aggregates.

a mixture of all the components in a 4 : 3 : 6 molar ratio for 1 h. The complex precipitates directly from the reaction mixture as a yellow solid in ~61% yield. The synthesis of **1** is summarized in eqn (1), considering the hydrolysis of one imine arm of the two ligands used in synthesis.

$$4H_3bemp + 3Zn(ClO_4)_2\cdot 6H_2O + 6NEt_3 \rightarrow [Zn_3(H_2bemp)_2(emp)_2] + 6(NHEt_3)(ClO_4) + 2NH_2(CH_2)_2OH + 16H_2O \quad (1)$$

The elemental analysis and molar conductivity data are consistent with the formula $[Zn_3(H_2bemp)_2(emp)_2]$ for **1**. The formula of **1** contains two H_2bemp^- ligands and two emp^{2-} ligands for a triangular Zn_3 aggregation. The *in situ* formed ligand emp^{2-} (Scheme 3, right) originates from the hydrolysis of one of the imine arms of H_3bemp, as assisted in all probability by the coordination of metal ions. Interestingly, such a hydrolysis reaction in the presence of metal ions is not a routinely observable pathway and is not observed as part of previously reported clusters obtained with H_3bemp.[18] However, no sign of the formation of hydroxide-phenoxide bridged partial dicubane **3** was observed (Scheme 4). This synthetic procedure was further explored with a related ligand H_3bpmp in place of H_3bemp. Orange single crystals of **2**·2H_2O (Scheme 4) from an orange reaction mixture were directly obtained in 36% yield in CH_3OH by stirring a reaction mixture of H_3bpmp, $Zn(ClO_4)_2\cdot 6H_2O$ and NEt_3 in a 2 : 1 : 2 molar ratio, following a few trials, for 10 min under aerobic condition at room temperature. The synthesis of **2**·2H_2O from H_3bpmp is summarized in eqn (2), considering the non-hydrolytic behavior of H_3bpmp and generation of zwitterions during the complexation reaction.

$$2H_3bpmp + Zn(ClO_4)_2\cdot 6H_2O + 2NEt_3 \rightarrow [Zn(H_2bpmpH^N)_2](ClO_4)_2\cdot 2H_2O + 2NEt_3 + 4H_2O \quad (2)$$

The elemental analysis and molar conductivity value establish the formula of **2**. The nature of the final complex is greatly influenced by the ligand used, specifically on the imine-alcohol arm length. The formation of **2**·2H_2O shows the incorporation of *in situ* generated zwitterions from H_3bpmp as H_2bpmpH^N following the transfer of a proton from the phenoxido oxygen to the adjacent imine nitrogen, which in turn could not bind the metal ion preventing full utilization of its metal binding ability. Under similar reaction conditions, H_3bemp and its analogue of H_3bpmp react differently with $Zn(ClO_4)_2\cdot 6H_2O$ to give **1** and **2**·2H_2O. The formation of double phenoxido bridged **3** was not achieved (Scheme 4), perhaps because of the additional stability of **2**·2H_2O, which crystallizes as a mononuclear complex of any binucleating ligand in zwitterionic form, showing tridentate coordination and dangling uncoordinated side arm, assembled through H-bonding. Following several synthetic trials in varying solvent systems and reaction conditions we failed to obtain the Zn_2 species **3** (Scheme 4). The proposal for the formation of **4** comes from our previous work on the binding of cobalt(II) ions as a Co_4 complex with H_3bemp. The nature of the final reaction product is greatly influenced by the choice of ligand, solvent system and the sequence of addition of the reactants.

All the compounds are insoluble in water and separate immediately from the reaction mixture. Elemental analysis, metal estimation, solution electrical conductivity and FTIR and UV-vis spectroscopic studies confirmed the formation of **1** and **2**·2H_2O. The molar conductivity values (Λ_M) in MeOH are 6 and 192 Ω^{-1} cm^2 mol^{-1} (at 32 °C) for **1** and **2**·2H_2O, respectively. The value for **2**·2H_2O corresponds to a 1 : 2 electrolyte behavior and indicate the stability of the mononuclear zinc(II) complex in solution.

Table 1 Crystallographic data for **1** and **2**·2H_2O

Compound	**1**	**2**·2H_2O
Formula	$C_{48}H_{56}N_6O_{12}Zn_3$	$C_{30}H_{46}Cl_2N_4O_{16}Zn$
Color	Yellow	Orange
M_r	1105.10	855.00
Space group	$C2/c$	$C2/c$
Crystal system	Monoclinic	Monoclinic
a/Å	13.956(2)	25.197(4)
b/Å	23.659(4)	11.2209(15)
c/Å	15.888(3)	16.045(2)
α (°)	90.00	90.00
β (°)	107.112(10)	121.446(4)
γ (°)	90.00	90.00
U/Å^3	5013.7(14)	3870.1(9)
T/K	293	293
λ(Mo-Kα)/cm^{-1}	0.71073	0.71073
Z	4	4
D_c/g cm^{-3}	1.464	1.467
Cryst. dimens./mm	0.36 × 0.29 × 0.16	0.36 × 0.22 × 0.18
F(000)	2288	1776
μ(Mo-Kα)/cm^{-1}	14.90	8.46
Measured reflns	11426	24987
Unique reflns	3208	4132
R_{int}	0.0822	0.0518
Obs. reflns $I \geq 2\sigma(I)$]	2173	2799
θ_{min}–θ_{max} (°)	3.05–22.50	1.89–26.81
hkl ranges	−15,15;−22,25;−17,17	−31,31;−14,14;−20,20
$R(F^2)$ (obs. reflns)	0.0710	0.0707
w$R(F^2)$ (all reflns)	0.1457	0.2147
No. variables	314	252
Goodness of fit	1.079	1.037
$\Delta\rho_{max}$; $\Delta\rho_{min}$/e Å^{-3}	0.371, −0.352	0.869; −0.715

Description of structure

Single crystals suitable for single-crystal X-ray structure determination were obtained by slow evaporation of a saturated MeOH solution of **1** and **2**·2H_2O after one week and 8 d, respectively. The crystallographic data are summarized in Table 1 and selected bond lengths and bond angles are collected in Table 2.

$[Zn_3(H_2bemp)_2(emp)_2]$ (1). Complex 1 forms yellow crystals belonging to the monoclinic crystal system, space group $C2/c$ (no. 15). A perspective view of $[Zn_3(H_2bemp)_2(emp)_2]$ (**1**) with the atom-numbering scheme is shown in Fig. 1. This is a discrete trinuclear complex having angular Zn2–Zn1–Zn2* disposition of 82°. The asymmetric unit of complex **1** consists of two Zn^{2+} ions and one each of H_2bemp^- and emp^{2-} (Fig. S1†). The complex next grows about the symmetry requirement of the space group with three Zn^{2+} ions, two H_2bemp^- and two hydrolyzed emp^{2-} ligands. The bridging within the V-shaped structure is ensured by two μ-H_2bemp^- and two μ_3-emp^{2-} moieties. Both alcohol arms of the ligand H_2bemp^- remain uncoordinated and engaged in hydrogen-bonding interactions with phenoxido oxygen atoms at 2.779 Å. Two μ-phenoxido (O1 and O1*) bridges provided by two H_2bemp^- connect three zinc atoms in angular fashion. The terminal μ-alkoxido (O4 and O4*) bridges between Zn1···Zn2 and Zn1···Zn2* come from the single alcohol arms of emp^{2-}. The molecule provides a new example of a Zn_3 complex of two types of coordination geometries around three metal ions. Atom

Table 2 Selected bond lengths (Å) and bond angles (°)[a] for complexes **1** and **2**·2H_2O

1			
Distances			
Zn(1)–O(1)	2.066(5)	Zn2–O4	1.963(5)
Zn(1)–O(4)	2.145(5)	Zn2– O5	2.010(7)
Zn(1)–N(2)	2.146(7)	Zn2– N1	2.064(7)
Zn1 ··· Zn2	3.1494(15)	Zn2– O1	2.140(5)
Angles			
O1–Zn1–O1[a]	159.5(3)	O4 –Zn2– N3	121.4(2)
O1– Zn1–O4	93.90(19)	O5– Zn2– N3	90.0(3)
O1– Zn1– O4[a]	72.20(19)	O4 –Zn2 –N1	120.2(2)
O4– Zn1– O4[a]	96.4(3)	O5– Zn2– N1	95.6(3)
O1– Zn1– N2[a]	110.2(2)	N3 –Zn2– N1	115.6(2)
O1 –Zn1– N2	84.8(2)	O4– Zn2 –O1	74.3(2)
O4 –Zn1– N2	92.4(2)	O5– Zn2– O1	174.3(2)
O4– Zn1– N2	155.8(2)	N3– Zn2– O1	95.3(3)
N2– Zn1– N2[a]	88.6(4)	N1 –Zn2– O1	84.1(3)
O4– Zn2 –O5	101.1(2)		
2·2H_2O			
Distances			
Zn(1)–O(1)	2.093(3)	Zn(1)–N(2)	2.103(4)
Zn(1)–O(2)	2.130(4)		
Angles			
O(1)–Zn(1)–O(1)[a]	92.89(18)	O(1)–Zn(1)–O(2)[a]	89.35(16)
O(1)–Zn(1)–N(2)[a]	92.13(14)	N(2)[a]–Zn(1)–O(2)[a]	90.47(17)
O(1)–Zn(1)–N(2)	84.39(14)	N(2)–Zn(1)–O(2)	90.47(16)
N(2)–Zn(1)–N(2)[a]	175.0(2)	N(2)–Zn–(1)O–(2)	93.13(16)
O(1)[a]– Zn(1)–O(2)[a]	174.46(15)	O(2)–Zn(1)–O(2)[a]	88.9(3)

[a] Symmetry code: $-x$, y, $1.5 - z$.

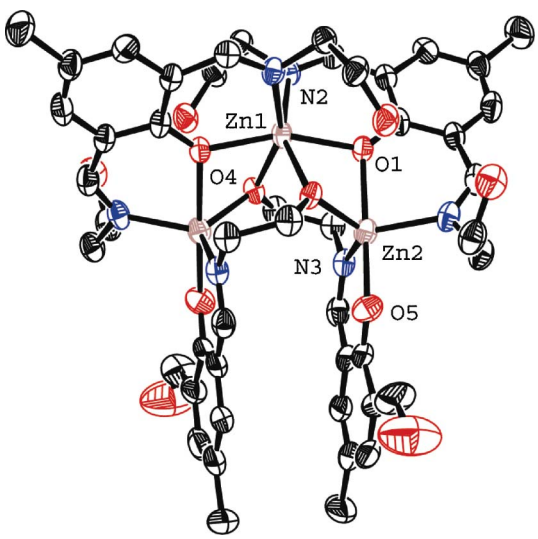

Fig. 1 Labeled ORTEP[20] view of [$Zn_3(H_2bemp)_2(emp)_2$] (**1**) with atom numbering scheme. Thermal ellipsoids for different atoms are drawn at the 30% probability level; H atoms are omitted for clarity.

Zn1 is hexacoordinated by two μ-phenoxido oxygen atoms (O1 and O1*) and two imine nitrogen atoms (N2 and N2*) of the ligands H_2bemp^-, and two μ-alkoxido oxygen atoms (O4 and O4*) of the ligands emp^{2-}. Hexacoordinated Zn1 adopts a distorted octahedral geometry (Fig. S2†) with *cis* angles ranging from 72 to 110° clearly demonstrating the amount of deformation. In contrast, Zn2 and its symmetry related Zn2* are joined by the μ-phenoxido and imine of one pocket of H_2bemp^- and a terminal phenoxido, imine and μ-alkoxido of emp^{2-}. The pentacoordinated Zn2 and Zn2* are in disorted TBP (trigonal bi-pyramidal) geometries with an addition parameter,[19] τ, of 0.88 ($\tau = [|\theta - \Phi|/60]$, $\tau = 0$ for perfect SP and 1 for ideal TBP geometries), and the Zn^{2+} ion is displaced by 0.19 Å towards O5 from the best trigonal plane formed by atoms N1, N3 and O4. Two axial distances (Zn2–O1 and Zn2–O5) from this plane are 2.140 and 2.011 Å, clearly indicating the shorter length for the non-bridging phenoxido oxygen atom (O5). It is quite obvious from the crystal structure of this complex that the three Zn^{2+} ions in the molecule have two different environments in their coordination spheres. The phenoxido bridge from O1 to Zn atoms is unsymmetrical at 2.066 and 2.140 Å from Zn1 and Zn2. Similarly the alkoxido bridge from O4 records distances of 1.963 and 2.145 Å from Zn2 and Zn1 (Fig. S3†). Thus the strongest Zn-O bond is provided by the alkoxido bridge at the 5-coordinated metal ion center. Two different coordination environments bring terminal zinc atoms close to the central atom through both phenoxido and alkoxido bridges (Fig. S4 in the ESI†). Like the Zn_3 motif in P1 nuclease, two of the Zn centres in **1** are in N_2O_3 coordination environments and the central Zn is in an octahedral N_2O_4 environment. Compared to P1 nuclease (Scheme 1) the Zn ··· Zn distances are shorter in the range of 3.149–4.149 Å. A zig-zag arrangement of Zn_3 motifs is seen in the packing diagram of **1** (Fig. S5†).

[$Zn(H_2bpmpH^N)_2$](ClO_4)$_2$·2H_2O (2·2H_2O). Complex **2**·2H_2O forms orange crystals and like **1** belongs to the monoclinic crystal system, space group $C2/c$ (no. 15). The ORTEP representation of the complex in Fig. 2 shows a mononuclear Zn^{II} cation that is six-coordinate in distorted octahedral geometry. The amount of distortion is less compared to complex **1**. The asymmetric unit of **2**·2H_2O consists of one Zn^{2+} ion and one neutral H_2bpmpH^N (Fig. S6†). The 6-coordinate Zn1 center is bound to two non-bridging phenoxido oxygen atoms, two imine nitrogen atoms and two alcohol oxygen atoms of two zwitterionic ligands H_2bpmpH^N. The Zn1 atom adopts a less distorted octahedral geometry compared to complex **1** (Fig. S7†) with *cis* angles ranging from 84 to 93°. The non-bridging phenoxido and protonated alcoholic oxygen atoms bind the metal center in *cis* positions. In *trans* dispositions the alcoholic oxygen atoms are at longer distance (2.130 Å) than the phenoxido oxygen atoms (2.093 Å). The ligands H_3bpmp, having the potential to bind two metal ions, within the present reaction condition, function as tridentate N_2O donor species due to the

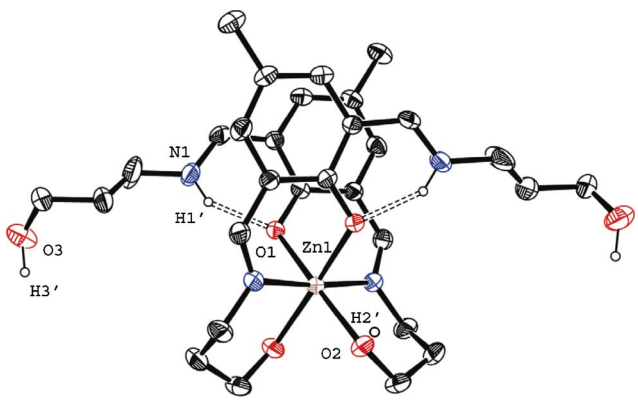

Fig. 2 Labeled ORTEP[20] representation of [$Zn(H_2bpmpH^N)_2$](ClO_4)$_2$·2H_2O (**2**·2H_2O) with atom numbering scheme and thermal ellipsoids drawn at the 30% probability level.

zwitterionic transformation of the other half not available for metal coordination. Single alcohol arms from each H_2bpmpH^N ligand remain uncoordinated and engaged in hydrogen-bonding interactions with lattice water oxygen atoms at 2.757 Å and nearby perchlorate anions. This arrangement is responsible for the stabilization of the pendant imine-alcohol arms of two ligands. The imine groups of the second arm are protonated and H-bonded to the Zn^{II} bound phenoxido oxygen atoms (N···O av. 2.571 Å, Fig. 2). This type of mononuclear coordination of any binucleating ligand to Zn^{II} is not known in the literature. The *b*-axis crystal packing diagram of **2**·2H_2O shows individual mononuclear units separated by dangling iminium-alcohol arms (Fig. S8 in ESI†).

FT-IR spectra. The broad and sharp peaks in the FTIR spectra of **1** at 3420 and 1636 cm^{-1} are due to the stretching modes characteristic of the uncoordinated ligand O–H and bound C=N functionalities of H_2bemp^- and emp^{2-}. For complex **2**·2H_2O the sharp peak at 1635 cm^{-1} is due to the $\nu_{C=N}$ stretching frequency of H_2bpmpH^N and a broad medium band at 3421 cm^{-1} for the ν_{OH} vibrations from the ligand O–H groups and lattice water molecules. It also contains the characteristic vibration at 1121 cm^{-1} for the uncoordinated perchlorate anions.[21]

Absorption study. The mode of coordination of H_3bemp and H_3bpmp with Zn^{2+} was investigated by absorption spectrophotometric titration at 25 °C in 10 mM HEPES buffer (pH 7.4). Fig. 3 illustrates a typical UV-vis titration curve of H_3bemp with added Zn^{2+}. The absorption intensity of H_3bemp at 430 nm gradually decreases as the concentration of Zn^{2+} increases stepwise. On further addition of the Zn(II) salt, the intensity of the band at 430 nm is diminished, while another new band at 353 nm is gradually generated with an isosbestic point 374 nm. This absorption peak is likely to be due to the binding of H_3bemp with Zn^{2+} in 1 : 1 molar ratio.[22] The zinc complexes are known to register only the charge transfer transitions as no d-d transitions are expected for a d^{10} Zn^{2+} ion.[23] This band at 353 nm may be associated with a $\pi \rightarrow \pi^*$ transition originating mainly in the azomethine chromophore (imine $\pi \rightarrow \pi^*$ transition). No more increase in the absorption of the band at 353 nm occurred following the addition of excess 1.0 equiv. of Zn^{2+}. The absorption spectral changes corresponding to the spectrophotometric titrations of H_3bpmp with $Zn(ClO_4)_2·6H_2O$ at 25 °C in 10 mM HEPES buffer (pH 7.4) are shown in Fig. S9.† The characteristic absorbance of H_3bpmp at 430 nm gradually decreases as the concentration of Zn^{2+} increases and a new band appears at 350 nm through an isosbestic point at 380 nm. Moreover, the absorption band at around 350 nm remains constant in the presence of more than 1 equiv. of Zn^{2+} ions, indicating the formation of a 1 : 1 complex between H_3bpmp and Zn(II).

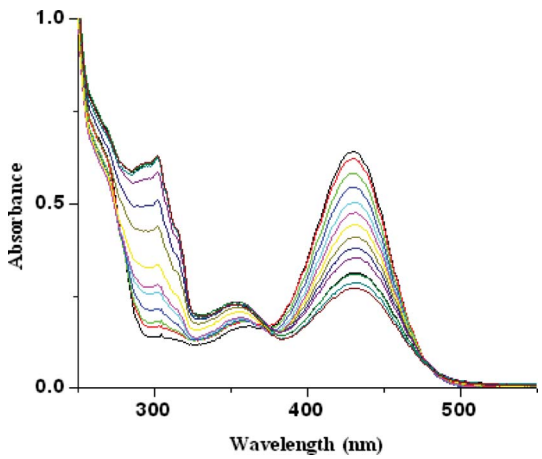

Fig. 3 Spectrophotometric titrations of H_3bemp (10 μM) with various numbers of equiv. of $Zn(ClO_4)_2·6H_2O$ in 10 mM HEPES buffer (pH 7.4) at room temperature ([Zn^{2+}] = 0, 1, 1.5, 2, 3, 4, 5, 6, 7, 8, 9, 10, 11 μM).

Fluorescence behavior. The emission spectra of the two ligands (10 μM of H_3bemp and H_3bpmp) used in this study record emission maxima in 10 mM HEPES buffer at 28 °C at 482 nm and 504 nm when the solutions are excited at 350 nm and 348 nm, respectively. The emission intensities of the binucleating chelator molecules were measured in the presence of various amounts of $Zn(ClO_4)2·6H_2O$ (0–11 μM). The system shows specific coordination induced emission behavior. The emission is maintained at 465 nm after addition of more quantities of Zn^{2+} following 1 : 1 coordination with Zn^{2+} as compared to that at 494 nm of the free ligand. The emission band of the free ligand is at longer wavelength compared to the metal–ligand system. The change in the emission maximum for H_3bemp during coordination with Zn^{2+} is shown in Fig. 4 (the same for H_3bpmp is given Fig. S10 of ESI†).

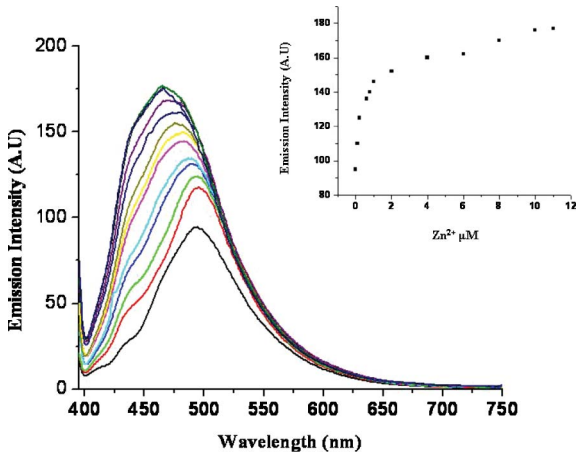

Fig. 4 Emission spectra of 10 μM of H_3bemp in the presence of 0, 0.1, 0.2, 0.6, 0.8, 1, 2, 4, 6, 8, 10, 11 μM of free Zn^{2+} ions in 10 mM HEPES buffer (pH 7.4) at room temperature (excitation 350 nm, emission 465 nm). Inset: fluorescent enhancement *vs.* different concentrations of Zn^{2+}.

For H_3bemp the fluorescence (emission of photon) quantum yield (Φ = no. of photons emitted/no. of photons absorbed = 0.201) was increased about 4-fold to 0.804 when one equiv. of Zn^{2+} was added to the ligand in MeOH at 28 °C. This quantum yield is essentially related to the emission efficiency of the 1 : 1 metal–ligand system, the fluorophore system in the present case, which did not result in the isolation of the hitherto unknown complex $[Zn_2(H_2bempH^N)_2](ClO_4)_2$. The incorporation of Zn^{2+} ions into H_3bemp lead to the modulation of the photophysical responses of the ligand by creating a suitable excited-state to register the observed emission behavior. The modified Benesi–Hildebrand equation: $1/\Delta F = 1/\Delta F\max + (1/K[C])(1/\Delta F\max)$ was used to establish the binding interaction of the ligand with Zn^{2+} and the binding constant value has been determined from the emission intensity data.[24] Here, $\Delta F_{max} = Fx - F_0$ and $\Delta F_{max} = F_\infty - F_0$,

where F_0, F_x and F_∞ are the emission intensities of the ligand used in the absence of Zn^{2+}, at an intermediate Zn^{2+} concentration, and at a concentration of complete interaction, respectively, and where K is the binding constant and $[C]$ the Zn^{2+} concentration. From the plot (Fig. 5) of $(F_\infty–F_0)/(F_x–F_0)$ against $[C]^{-1}$ for H_3bemp, the value of K extracted from the slope is 4.5×10^3 M^{-1}. When a 2.0×10^{-5} M solution of the isolated **1** in 10 mM HEPES buffer is excited at 350 nm, it emits at 501 nm with quenching of intensity compared to the *in situ* generated complex with H3bemp. The process can be considered as a Zn^{2+} ion chelation induced fluorescence enhancement for H_3bemp. In the case of **2**·$2H_2O$, a 1.0×10^{-5} M solution in 10 mM HEPES buffer emits at 493 nm when excited at 348 nm and binding constant value K extracted from the slope is 4.2×10^3 M^{-1} (Fig. S11†).

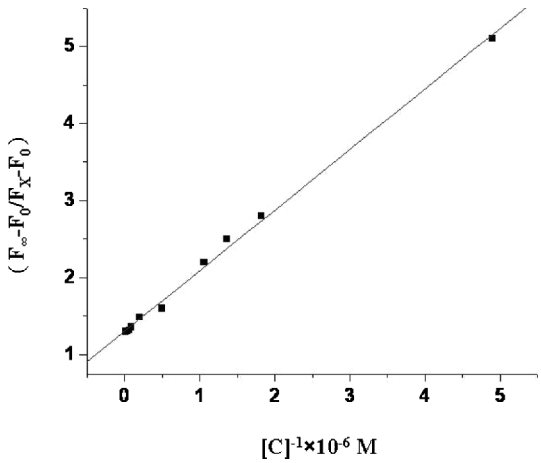

Fig. 5 Extraction of the binding constant from a modified Benesi–Hildebrand plot.

Different anions (*e.g.*, perchlorate, chloride, nitrate, acetate *etc.*) available as Zn^{2+} salts have almost no effect on the emission intensity when these salts are added to the ligand (Fig. S12 of ESI†). In the case of **2**·$2H_2O$ though there is a scope for the replacement of ClO_4^- anions by the above indicated anions but fluorescence measurements are insensitive to anion replacement, if any. Job's plot analysis revealed maximum emission at 1 : 1 ratio (ligand : Zn^{2+}) (Fig. S13†).

The fluorescence quantum yields of H_3bemp, H_3bpmp, **1** and **2**·$2H_2O$ were measured relative to quinine sulfate as the secondary fluorescence standard, and are calculated on the basis of eqn 3,[25]

$$\frac{\Phi_S}{\Phi_R} = \frac{A_S}{A_R} \times \frac{(Abs)_R}{(Abs)_S} \times \frac{n_S^2}{n_R^2} \quad (3)$$

where Φ is the quantum yield, Abs is absorbance, A is the area under the fluorescence curve, and η is the refractive index of the medium. The subscripts S and R denote the corresponding parameters for the sample and reference, respectively. The fluorescence quantum yields of the different species are given in Table 3. We have also examined the change in emission behavior on addition of other metal ions. H_3bemp and H_3bpmp show analogous behavior towards other metal ions. Metal ion binding selectivity was assayed in 10 mM buffer HEPES with excitation at 350 nm. Fig. 6 shows the fluorescence intensities of H_3bemp (1.0×10^{-5} M) in the presence of different metal ions.

Table 3 Fluorescence quantum yields[a] of the ligands and their complexes with Zn(II)

System	Absorption maximum/nm	Emission maximum/nm	Fluorescence quantum yield
H_3bemp	450	497	0.201
H_3bpmp	450	498	0.160
1	385	488	0.052
2·$2H_2O$	410	498	0.094
H_3bemp+Zn(1 : 1)	385	465	0.804
H_3bpmp+Zn(1 : 1)	410	504	0.301

[a] The fluorescence quantum efficiency was determined by using quinine sulfate as reference ($\Phi_R = 0.54$).

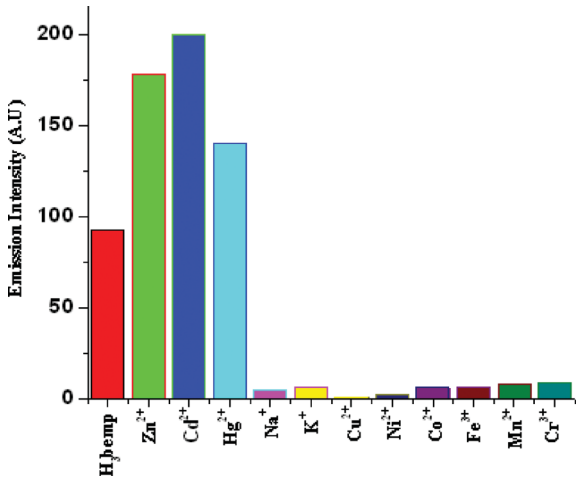

Fig. 6 Relative fluorescence intensity change of H_3bemp (1.0×10^{-5} M) in the presence of various metal ions at room temperature (excitation at 350 nm).

For H_3bpmp the same is given in Fig. S14 of ESI.† It is observed that among the metal ions studied; only Zn^{2+}, Cd^{2+} and Hg^{2+} efficiently change the emission behavior of both the ligands, though Hg^{2+} is well known as a typically quenching metal ion.[26] Other biogenic cations, known to be present at high concentrations in living cells, *e.g.*, Na^+ and K^+, do not enhance the emission intensity as shown in Fig. 6, most probably due to the meager complexation potential of alkali metal ions with the ligands. The UV-vis spectra also do not record any change upon addition of these two metal ions and do not interfere with the Zn^{2+} triggered fluorescence enhancement. Other metal ions such as Cr^{3+}, Mn^{2+}, Fe^{3+}, Co^{2+}, Ni^{2+} and Cu^{2+} quench the emission intensities following the addition of upto 3 equiv. of these cations. This is due to an electron and energy transfer between the metal cation and fluorophore ligand known as the fluorescence quenching mechanism responsible to yield a strong quenching response.[27,28] These metal ions can interfere with the fluorescent signal of the ligands in detecting other metal ions and fluorescence quenching can be caused by number of factors and as a result can be nonspecific.

Solid state thermal decomposition behavior. The compositional changes of the two compounds associated with the calcination process were followed using thermogravimetric analysis (TGA). It shows that both the metal complexes can be converted to a ZnO phase *via* solid-state transformation. The typical TGA curves were

recorded in a static atmosphere of nitrogen at a heating rate of 10° min^{-1} between 30–850 °C. The compound **1** is stable up to 275 °C (Fig. S15 in the ESI†) and showed sharp single-step decomposition in the temperature range 230–340 °C, assigned to the loss of the four Schiff base fragments (~39.8% weight loss). For **2**·2H_2O (Fig. S15 in the ESI†) loss of water starts ~78.7 °C and completes at 96.75 °C. The observed loss of weight is 3.246%, which agrees well with the calculated value of 4.2% for two water molecules.

X-Ray crystallography

The intensity data of the complexes **1** and **2**·2H_2O were collected on a Nonius Kappa CCD and Bruker APEX-II CCD X-ray diffractometer that uses graphite-monochromated Mo-Kα radiation ($\lambda = 0.71073$ Å) at 293 K, using single crystals. Information concerning the X-ray data collection and structure refinement of the compound is summarized in Table 1. For complex **1**, a total of 3208 reflections were recorded with Miller indices $h_{min} = -15$, $h_{max} = 15$, $k_{min} = -22$, $k_{max} = 25$, $l_{min} = -17$, $l_{max} = 17$. For complex **2**·2H_2O, a total of 4132 reflections were recorded with Miller indices $h_{min} = -31$, $h_{max} = 31$, $k_{min} = -14$, $k_{max} = 14$, $l_{min} = -20$, $l_{max} = 20$. In the final cycles of full-matrix least squares on F^2 all non-hydrogen atoms were assigned anisotropic thermal parameters. The structures were solved using SIR97 and SHELX-97[29] system of programmes.

Conclusions

We have investigated the fluorescence and binding behavior of H_3bemp and H_3bpmp with Zn^{2+}. In solution they indicate selectivity for Zn^{2+} in comparison to other metal ions and zinc ion coordination selective fluorescence properties. With H_3bemp, the neutral Zn_3 nuclearity in the form of a compact triangle has been achieved in **1** as a single crystalline end product by the combined action of singly deprotonated parent H_2bemp^- and its hydrolyzed form emp^{2-}. The combined effect of the two ligands, one derived from the other, introduces phenoxido and alkoxido bridging moieties. The fluorescent coordinative interaction of the second ligand, also selective towards the Zn^{2+} ion, instead leads to the generation of mononuclear **2**·2H_2O of two zwitterionic ligands. In addition, the trinuclear and mononuclear zinc(II) complexes reported can function as precursors for the preparation of ZnO nano structures.

Acknowledgements

A.S. is thankful to the University Grant Commission, New Delhi, India for the research fellowship. The authors also give thanks to DST, New Delhi, for providing the Single Crystal X-ray Diffractometer facility in the Department of Chemistry, IIT Kharagpur under its FIST program. V.B. acknowledeges Italian Ministry of University and Scientific Research, MIUR, Rome, Italy.

Notes and References

1 (*a*) M. Sarkar, R. Clérac, C. Mathoniére, N. G. R. Hearns, V. Bertolasi and D. Ray, *Inorg. Chem.*, 2010, **49**, 6575; (*b*) M. Sarkar, R. Clérac, C. Mathoniére, N. G. R. Hearns, V. Bertolasi and D. Ray, *Inorg. Chem.*, 2011, **50**, 3922.
2 (*a*) S. Khanra, S. Konar, A. Clearfield, M. Helliwell, E. J. L. McInnes, E. Tolis, F. Tuna and R. E. P. Winpenny, *Inorg. Chem.*, 2009, **48**, 5338; (*b*) C. Lampropoulos, K. A. Abboud, T. C. Stamatatos and G. Christou, *Inorg. Chem.*, 2009, **48**, 813; (*c*) A. Escuer, G. Vlahopoulou, S. P. Perlepes and F. A. Mautner, *Inorg. Chem.*, 2011, **50**, 2468.
3 A. Volbeda, A. Lahm, F. Sakiyama and D. Suck, *EMBO J.*, 1991, **10**, 1607.
4 (*a*) E. Hough, L. K. Hansen, B. Birkens, K. Jynes, S. Hansen, A. Hordvik, C. Little, E. Dodson and Z. Derewenda, *Nature*, 1989, **338**, 357; (*b*) S. K. Burley, P. R. David, R. M. Sweet, A. Tayler and W. N. Lipscomb, *J. Mol. Biol.*, 1992, **224**, 113.
5 (*a*) E. E. Kim and H. W Wyckoff, *J. Mol. Biol.*, 1991, **218**, 449; (*b*) A. P. Cole, D. E. Root, M. Mukherjee, E. I. Solomon and T. D. P. Stack, *Science*, 1996, **273**, 1848.
6 (*a*) A. I. Bush, *Curr. Opin. Chem. Biol.*, 2000, **4**, 184; (*b*) S. W. Suh, J. W. Chen, M. Motamedi, B. Bell, K. Listiak, N. F. Pons, G. Danscher and C. J. Frederickson, *Brain Res.*, 2000, **852**, 268; (*c*) D. W. Choi and J. Y. Koh, *Annu. Rev. Neurosci.*, 1998, **21**, 347.
7 M. Fondo, N. Ocampo, A. M. Garca-Deibe and J. Sanmartin, *Inorg. Chem.*, 2009, **48**, 4971.
8 (*a*) J. J. Danford, P. Dobrowolski and L. M. Berreau, *Inorg. Chem.*, 2009, **48**, 11352; (*b*) A. A. Russell, K. Doyle, A. M. Arif and L. M. Berreau, *Inorg. Chem.*, 2006, **45**, 4097.
9 L. A. Gavrilova and B. Bosnich, *Chem. Rev.*, 2004, **104**, 349.
10 (*a*) D. Mandal and D. Ray, *Inorg. Chem. Commun.*, 2007, **10**, 1202; (*b*) S. S. Tandon, D. S. Bunge, R. Rakosi, Z. Xu and L. K. Thompson, *Dalton Trans.*, 2009, 6536.
11 D. Mandal, V. Bertolasi, J. R. Ariño, G. Aromí and D. Ray, *Inorg. Chem.*, 2008, **47**, 3465.
12 N. L. William and S. Norbert, *Chem. Rev.*, 1996, **96**, 2375.
13 (*a*) T. K. Cole and R. G. Linck, *Inorg. Chem.*, 1988, **27**, 1498; (*b*) D. E. Fogg and B. R. James, *Inorg. Chem.*, 1995, **34**, 2557.
14 A. Tamilselvi and M. Govindasamy, *JBIC, J. Biol. Inorg. Chem.*, 2008, **13**, 1039.
15 R. S. Forgan, J. E. Davidson, S. G. Galbraith, D. K. Henderson, Parsons, S. Parsons, P. A. Tasker and F. J. White, *Chem. Commun.*, 2008, 4049.
16 R. R. Gagne, C. L. Spiro, T. J. Smith, C. A. Hamann, W. R. Thies and A. K. Shiemke, *J. Am. Chem. Soc.*, 1981, **103**, 4073.
17 W. X. Zhang, C. Q. Ma, X. N. Wang, Z. G. Yu, Q. J. Lin and D. H. Jiang, *Chin. J. Chem.*, 1995, **13**, 497.
18 B. J. Hathaway, G. Wilkinson, R. G. Gillard and J. A. McCleverty, ed., *Comprehensive Coordination Chemistry*, Pergamon Press, Oxford, U.K., 1987, Vol. 2, p 413.
19 W. A. Addison, T. N. Rao, J. Reedijk, J. V. Rijn and G. C. Verschoor, *J. Chem. Soc., Dalton Trans.*, 1984, 1349.
20 M.N. Burnett, C.K. Johnson, ORTEP III, Report ORNL-6895, Oak Ridge National Laboratory, Oak Ridge, TN, 1996.
21 A. R. Paital, V. Bertolasi, G. Aromí, J. R. Ariño and D. Ray, *Dalton Trans.*, 2008, 861.
22 M. Prabhakar, P. S. Zacharias and S. K. Das, *Inorg. Chem.*, 2005, **44**, 2585.
23 (*a*) C. L. Dollberg and C. Turro, *Inorg. Chem.*, 2001, **40**, 2484; (*b*) D. M. Roundhill, *Photochemistry and Photophysics of Metal Complexes*, J. P. Fackler, ed., Modern Inorganic Chemistry Series, Plenum Press, New York, 1994, p 56.
24 (*a*) A. Mallick and N. Chahattopadhyay, *Photochem. Photobiol.*, 2005, **81**, 419; (*b*) H. A. Benesi and J. H. Hildebrand, *J. Am. Chem. Soc.*, 1949, **71**, 2703; (*c*) N. J. Turro, *Modern Molecular Photochemistry*, Benjamin Cummings Publishing Co., Inc., Menlo Park, CA, 1978.
25 J. R. Lakowicz, *Principles of Fluorescence Spectroscopy*, 2nd ed., Kluwer Academic/Plenum, New York, 1999.
26 S. S. Tan, S. J. Kim and E. T. Kool, *J. Am. Chem. Soc.*, 2011, **133**, 2664.
27 S. Banthia and A. Samanta, *J. Phys. Chem. B*, 2002, **106**, 5572.
28 S. Banthia and A. Samanta, *J. Phys. Chem. B*, 2006, **110**, 6437.
29 (*a*) A. Altomare, M. C. Burla, M. Camalli, G. L. Cascarano, C. Giacovazzo, A. Guagliardi, A. G. Moliterni and R. J. Spagna, *Appl. Crystallogr.*, 1999, **32**, 115; (*b*) G. M. Sheldrick, *SHELX-97, Program for Crystal Structure Refinement*, University of Göttingen, Germany, 1997.

